



Characterization and adsorption capacity of four low-cost adsorbents based on coconut, almond, walnut, and peanut shells for copper removal

Abderrahim Kali¹ · Abdelouahed Amar¹ · Ilyasse Loulidi¹ · Maria Jabri¹ · Chaimaa Hadey¹ · Hassane Lgaz² · Awad A. Alrashdi³ · Fatima Boukhelifi¹

Received: 22 December 2021 / Revised: 28 February 2022 / Accepted: 5 March 2022 / Published online: 20 March 2022
© The Author(s), under exclusive licence to Springer-Verlag GmbH Germany, part of Springer Nature 2022

Abstract

Agricultural wastes (AWs) are available abundantly at no or low costs; however, in most cases, not used reasonably. Despite their interesting chemical properties, coconut shells (CS), almond shells (AS), walnut shells (WS), and peanut shells (PS) are usually burned in the fields or discharged without any valorization. These AWs were investigated as low-cost bio-adsorbents to remove copper ions (Cu^{2+}) from aqueous solutions. The four adsorbents were characterized using X-ray diffraction (XRD), the Fourier transform infrared spectra (FTIR), nitrogen adsorption/desorption measurements, scanning electron microscopy, and energy-dispersion X-ray spectroscopy (SEM–EDS). Characterization results revealed that the materials under investigation had porous surfaces, rich in fibers, and several potential adsorption sites. Therefore, their adsorption capacity for Cu^{2+} removal was evaluated under different operating conditions. Results showed that the CS had the best adsorption capacity among tested AWs. Under optimized parameters, the highest adsorption capacity was found 25, 18, 10, and 5 mg/g for WS, CS, PS, and AS, respectively. The adsorption of Cu^{2+} on the four adsorbents followed the second-order rate equation and the Langmuir adsorption isotherm model. After the adsorption process, the characterization of studied materials revealed no structural changes, proving the physical adsorption of Cu^{2+} on shells through long-range interactions between Cu^{2+} and reactive sites of adsorbents. The high adsorption capacity of the selected adsorbent was attributed to the presence of high content of cellulose compared to lignin.

Keywords Copper adsorption · Agricultural waste · Coconut shell · Almond shell · Walnut shell, Peanut shell

1 Introduction

Different industrial sectors use heavy metals in various applications because of their interesting properties, such as the high electrical conductivity. However, these heavy

metals are toxic and one of the deadly contaminants in groundwater [1–4]. Even at low levels, their toxicity can lead to several effects on the nervous system, carcinogenic effects on the blood and bone marrow, and kidney disorders. Various metal ions are present in industrial wastewater. Therefore, properly treating this wastewater before discharge into the water bodies is a high priority globally [5–11].

Many water pollution control methods and techniques have been developed in recent years. Among these techniques are chemical precipitation processes, ion exchange, electrolysis, membrane processes, adsorption, etc. [12–17]. The adsorption process is one of the methods that have shown significant profitability for the elimination of contaminants of different natures, in particular organic pollutants (pesticides, dyes, phenolic compounds, etc.), and heavy metals (cadmium, lead, mercury, etc.) [15, 18–21]. Activated carbon adsorption is the most widely used and recommended process for

✉ Awad A. Alrashdi
aarashdi@uqu.edu.sa

✉ Fatima Boukhelifi
f.boukhelifi@umi.ac.ma

¹ Laboratory of Chemistry and Biology Applied To the Environment, Moulay Ismail University, BP 11201 Meknes, Morocco

² Department of Architectural Engineering, Hanyang University-ERICA, 1271 Sa 3-dong, Sangnok-gu, Ansan 15588, Republic of Korea

³ Chemistry Department, Umm Al-Qura University, Al-Qunfudah University College, Mecca, Saudi Arabia

treating wastewater in industries. Despite its effectiveness, activated carbon remains an expensive material and is imported most. Therefore, the research and development of new natural, abundant, economically profitable, and effective adsorbents for the treatment of ecosystems is a must. Nowadays, new regulations have emerged in environmental protection, particularly in the depollution and recycling of heavy metals that require environmentally friendly depollution procedures. When considering depollution of heavy metals by adsorption process, the use of low-cost natural adsorbents represents a good choice [7, 22–26]. Bio-adsorbents such as biomass, agricultural solid waste, and modified or unmodified clays have shown promising results for the adsorption of pollutants [27, 28].

Thanks to their natural abundance and affinity for heavy metals, agricultural wastes are an important option for removing heavy metals from aqueous solutions, which can be an excellent alternative to activated coal [29–31]. The agricultural waste provides a complex mixture containing lignin and cellulose as the main constituents. The adsorption of pollutants can occur through lignin's polar functional groups, including alcohols, aldehydes, ketones, acids, phenolic hydroxides, and ethers that can act as binding agents [32]. The adsorption treatment of Cu^{2+} in wastewater using agricultural wastes or biomass has been extensively studied [33–36]. Biomass is any type of wood-rich waste. There are two types of agricultural wastes. The waste of living organisms such as seafood and waste of plants such as biomass. Previous studies showed that seafood waste could be effective adsorbents for Cu^{2+} removal from aqueous solutions [37]. These studies showed that the elimination of Cu^{2+} could reach up to 90%, as in the case of raw chitin [38], due to the presence of lone electron pair on nitrogen of amine function [39]. Besides, several adsorbents from agricultural waste have been used for heavy metals removal from aqueous solutions such as carrot residues [40], soybean husks, cotton seed husks, rice straw, and bagasse [41], apple waste [42], banana marrow [43], peanut shells [44], grape stalks [45], wheat shell [46], tea waste [47], sunflower stalk [48], tree fern [49], *Capsicum annum* seeds [50], and palm kernel fibers [51].

It is paramount for life on Earth to valorize different natural wastes, given their actual or potential usefulness as renewable natural resources. Many aspects of human activity are dependent on these resources. In Morocco, particularly in the Meknes region, despite the substantial works related to agro-wastes valorization, these wastes are heavily discharged without any treatment. One of the main ways to effectively valorize these wastes is their integration into the economic cycle. In this regard, our research team aims to create, through research, a

complete valorization cycle that take into consideration academic research and local communities, and the present research is a one step towards achieving this goal. Furthermore, from a scientific point of view, although several research have been performed using agro-wastes, such as the batch removal of Cu^{2+} ions from aqueous solution using low cost adsorbents such as walnut, hazelnut, and almond shells under different experimental conditions [52], to the best knowledge of authors, no work is reported comparing the adsorption capacity of coconut, almond, walnut, and peanut shells for Cu^{2+} removal. Most of the reported results focus on the individual performance of agro-wastes or comparison with other adsorbents without a complete valorization program.

The present work reports a comparative study and critical analysis of Cu^{2+} adsorption on four types of agricultural wastes. The removal of Cu^{2+} from an aqueous solution by adsorption was carried out using coconut, almond, walnut, and peanut shells. Tested materials were characterized using X-ray diffraction (XRD), the Fourier transform infrared spectra (FTIR), nitrogen adsorption/desorption measurements, and SEM/EDS analysis. Then, the kinetic and isothermal study was undertaken. To get more insights about the adsorption mechanism, investigated materials were characterized after the adsorption process.

2 Materials and methods

2.1 Preparation of adsorbents

In Morocco, several regions are known for their high production of nuts, such as almond shells and walnut shells. The waste from these dry fruits is still discharged without any valorization at the regional or national level. The studied biomass samples were collected from different regions of Morocco: almond shells and coconut shell (Meknes), walnut shells (Marrakesh), and peanut shell (El Gharb). Collected shells were cut into small pieces and, after drying and crushing, washed thoroughly with double-distilled water. Then, the four biomass samples were dried in an oven for 24 h at 105 °C to reduce their moisture content. The cleaned shells were crushed and sieved to obtain particle size in the range of 1–5 mm. Investigated samples are shown in Figure S1, supplementary material.

2.2 Characterization of adsorbents

Fourier transform infrared spectroscopy is based on the analyzed material's absorption of infrared radiation ($400\text{--}4000\text{ cm}^{-1}$). It allows via the detection of characteristic vibrations to identify the chemical functional groups.

The FTIR spectra were collected using Shimadzu spectrometer (JASCO 4100, Japan). The structural analysis by X-ray diffraction (XRD) was carried out on a diffractometer type X-RD-6100-Shimadzu ($\lambda_{\text{Cu}} = 1.54 \text{ \AA}$). The diffraction spectrum was produced for 2θ value between 2° and 80° , at a scanning speed of $1^\circ/\text{min}$. The morphology of the biomass samples was studied using the Hitachi S-3400 N scanning electron microscope, equipped with an energy dispersion spectroscopy (SEM–EDS) probe.

2.3 N₂ adsorption measurement

Physical gas adsorption is a widely used method to study the porosity of solids. The specific surface of investigated samples was determined by gas multilayer adsorption, according to Brunauer, Emmett, and Teller (BET). Prior to measurements, for each sample, degassing process was performed for 16 h under vacuum at 350°C . The BET surface area was determined by a volumetric adsorption apparatus by nitrogen adsorption at -196°C using Micromeritics TriStar II.

2.4 Adsorption experiments

For batch adsorption experiments, tests were performed by adding specific amounts of each shell as adsorbent to Erlenmeyer flasks containing metal ion solutions and stirred at 180 rpm until equilibrium. The following experimental conditions were maintained: The temperature and pH were maintained at 25°C and $\text{pH} = 5.5$, respectively; a mass $m = 50 \text{ mg}$ of adsorbent, 20 mL of a solution of copper sulfate of concentration $C = 4 \times 10^{-3} \text{ mol/L}$. After a determined contact time, samples were filtered, and the final Cu^{2+} concentrations were measured. After the adsorption time (t), the filtrate was allowed to react with ammonia to form a complex to determine the residual concentration of Cu^{2+} by atomic absorption spectrophotometry (Perkin Elmer SIMAA 6000). The effect of initial Cu^{2+} concentration was investigated for isothermal study.

The removal rate $R(\%)$ and equilibrium adsorption capacity q_e (mg/g) were calculated using the following equations [25]:

$$R(\%) = \frac{C_0 - C_e}{C_0} \times 100 \quad (1)$$

$$Q_e \left(\frac{\text{mg}}{\text{g}} \right) = \frac{C_0 - C_e}{C_0 * m} \times V \quad (2)$$

where C_0 is the initial Cu^{2+} concentration (in mg/L) and C_e is the Cu^{2+} concentration at equilibrium (in mg/L).

Kinetic and isotherm models analyzed in the present work are listed in Table S1 along with their equations and fitting parameters.

3 Results and discussion

3.1 Characterization of adsorbents

3.1.1 FTIR analysis

Figure 1 shows the FTIR spectra illustrating the functional groups of different tested biomass samples. It can be noticed that all biomass samples have similar aromatic and aliphatic functional groups. These groups are the characteristics of three main constituents of the tested wastes, i.e., cellulose, hemicellulose, and lignin. These three components are mainly alkenes, esters, ketones, aromatic rings and alcohol, with different functional groups. Peaks located at $3400\text{--}2900 \text{ cm}^{-1}$ can be assigned to hydroxyl/aliphatic hydrocarbons, with prominent peaks at 3400 cm^{-1} (O–H), and 2900 cm^{-1} (C–H) [53]. The absorption peaks observed at $1765\text{--}1715 \text{ cm}^{-1}$ can be attributed to the aromatic C=O functional group, while those at 1270 cm^{-1} and $\sim 1050 \text{ cm}^{-1}$ are mainly associated with C–O–C and C–O–H, respectively [54, 55].

3.1.2 X-ray diffraction

Waste materials' crystalline and amorphous properties can be evaluated using XRD [56]. Because of their natural function of protecting the seed, shells are the hard raw material with a high crystallinity [57]. In this work, X-ray analysis was performed for biomasses to investigate their crystallinity [58]. Figure S2 (Supplementary material) shows the XRD curves of four biomasses. This analysis indicates two slightly narrow peaks detected at 2θ values around 16°C and 22°C for agricultural wastes. These peaks are due to the crystalline structure of the cellulose contained in the biomasses [59, 60]. Similar results were found in [61].

3.1.3 SEM–EDS analysis

The morphological and structural properties of biomasses were examined using the SEM–EDS, which provides morphological and elemental qualitative information. The inspection of AS and WS shows that they exhibit a different surface morphology (Fig. 2). From the SEM images of the biomasses, it can be noticed that both shells have a rough surface due to presence of pores. The WS (Fig. 2a) has a characteristic of a material with a rough and laminated structure. However, the surface morphology of AS (Fig. 2b) seems to have a less porosity with a more compact and smoother surface.

The EDS analysis at a specific location provides localized elemental analysis data. Therefore, it would be inappropriate

Fig. 1 FTIR spectra of biomass samples

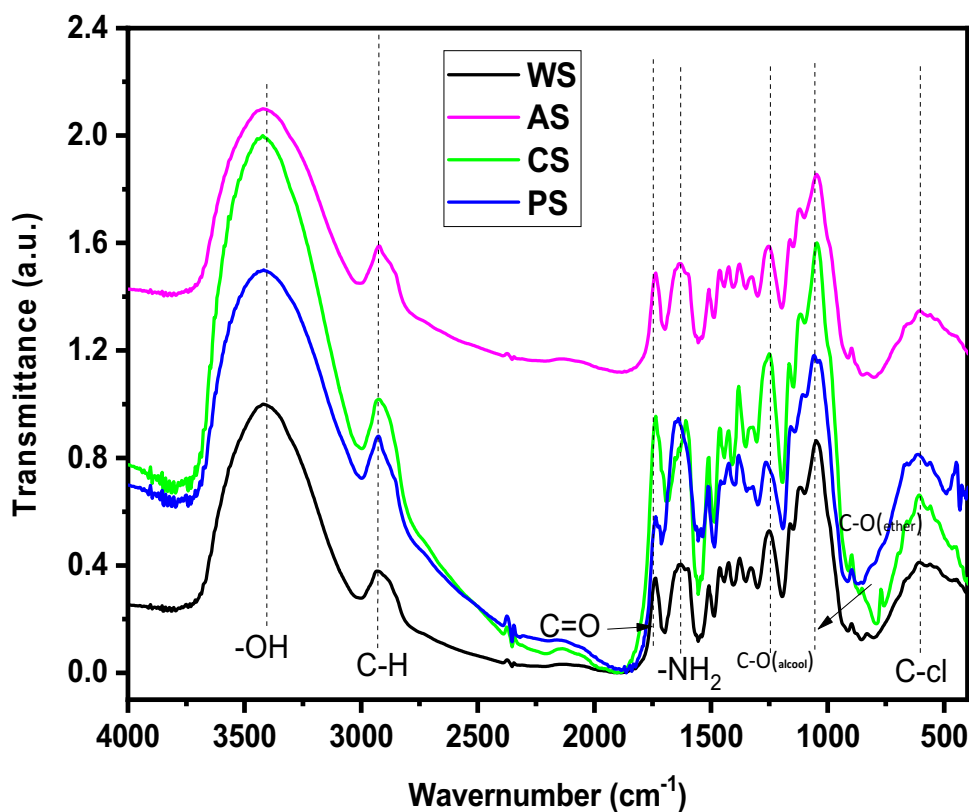


Fig. 2 SEM images of walnut shells and almond shells

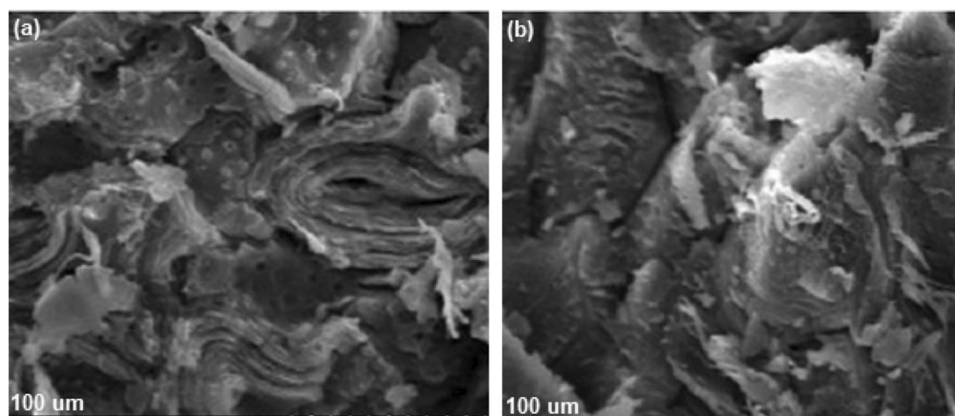


Table 1 EDS analysis of samples

Samples	C (wt%)	O (wt%)
AS	27	68.36
WS	26.94	68.21
CS	24.48	64.21
PS	23.92	69.4

to compare it with the basic analysis in bulk. However, EDS analysis (Table 1; Figure S3) reveals that all samples have a large amount of C and O. AS and WS have a bit higher carbon than other samples. In contrast, the PS has the highest amount of oxygen in the analyzed location. Traces of other

elements such as Ca, K, Al, and Mg are also detected in the biomass samples but very small amounts.

3.1.4 BET surface area measurements

The specific samples' areas are determined using the BET model and reported in Table 2. Specific surface area results of samples show that the CS has a clearly important surface compared to other shells, which can be attributed to the fibrous nature of the CS and spaces that separate its fibers. In contrast, walnut and almond shells have a compact structure, explaining the small decrease in their surface area. The specific surface area of the nut shells is similar to that found

Table 2 Surface area of samples obtained by BET theory

Samples	Surface area (m ² g ⁻¹)
AS	169.55
WS	148.08
CS	189.05
PS	176.05

by Ahmadou et al. [62, 63] in their work on three biochar’s derived from nut shells.

3.1.5 The pH at the zero-charge point

The point of zero charge (PZC) is an essential characteristic for surfaces because it represents an estimate of its acid–base. By definition, in the case where no specific sorption occurs (no surface complexation), the PZC corresponds to the pH of the medium for which the net proton charge equals Zero [64, 65]. The more the pH increases towards PZC, the more the density of negative ions on the surface of the adsorbent increases in turn, further allowing the adsorption of cations. According to Figure S4, the intersection point corresponds to a pH_{pzc} = 4.75, 4.86, 5.13, and 5.22 for AS, CS, WS, and PS, respectively. Therefore, at pH values lower than these points, the global charge of the adsorbent’s surface is positive and negative at pH values higher than these values. Considering our experimental conditions, at chosen pH (5.5), the adsorbent’s surface will have a negative charge, allowing positive metal cations to interact with it physically.

3.2 Copper ion adsorption

3.2.1 Contact time

It is of paramount importance in adsorption studies to investigate retention kinetics, which provides insights about the necessary contact time to achieve the adsorption equilibrium. The Cu²⁺ adsorption on the four tested samples is conducted, and results of adsorption capacity as function of contact time are shown in Fig. 5. The curves in Fig. 3 show that the kinetics of adsorption of Cu²⁺ on the various adsorbents is initially very fast, then starts to stabilize at *t* ≈ 80 min of contact, and finally fully stabilized at *t* = 180 min. The higher Cu²⁺ adsorption rate at the beginning is mainly due to the larger surface area of shells available for adsorbing Cu²⁺. When the surface adsorption sites become exhausted, the Cu²⁺ adsorption rate is controlled by the rate at which the adsorbate is transported from the exterior to the interior sites of the adsorbent particles [66]. On the other hand, at *t* = 120 min, the four materials represent the maximum adsorption capacity; therefore, it is designated

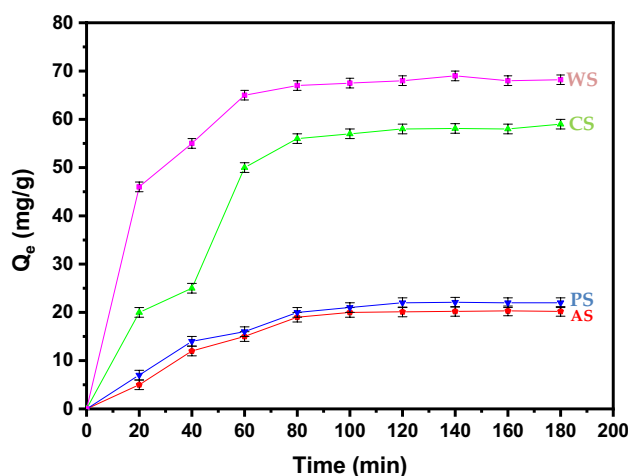


Fig. 3 Influence of contact time on copper adsorption on adsorbent supports: C₀ = 4 × 10⁻³ M, pH = 5.5, V_{sol} = 20 mL, m_{ads} = 50 mg, T = 25 °C

as the equilibrium time. The saturation value of the surface is 65.10 mg/g, 57.39 mg/g, and 26.14 mg/g, and 24.20 mg/g, for WS, CS, PS, and AS, respectively; in the following order: WS > CS > PS > AS. The difference in adsorption capacity between tested adsorbents is probably due to the diffusion rate and interaction strength of Cu²⁺ with each adsorbent’s surface. Although tested shells have a similar composition, their structures are different as shown from BET analysis. Similar behavior was observed in our previous study on Cu²⁺ adsorption on a natural bio-adsorbent [38].

3.2.2 Adsorption kinetics

Kinetic studies are useful for evaluating the adsorption mechanism [67, 68]. Kinetic studies were carried out using 50 mg of each adsorbent, 4 × 10⁻³ mol/L of Cu²⁺ in 20 mL of solution at pH = 5.5 and 25 °C temperature. The modeling of adsorption kinetics of Cu²⁺ has been investigated using pseudo-first-order (PFO) kinetic equation (Lagergren model) and pseudo-second-order (PSO) (Ho et McKay model) [69, 70]. The expression of the PFO equation is as follows:

$$\frac{dQ_t}{dt} = k_1(Q_e - Q_t) \tag{3}$$

where *Q_e* in mg/g is the amount of Cu²⁺ adsorbed at equilibrium, while *Q_t* in mg/g, the amount of Cu²⁺ adsorbed at the moment (*t*). The *k₁* is the PFO rate constant (min⁻¹).

The following expression describes the PSO equation:

$$\frac{dQ_t}{dt} = K_2(Q_e - Q_t)^2 \tag{4}$$

where *k₂* is the PSO’s rate constant in g/mg min.

The PFO kinetic model suggests that “the rate of sorption is proportionally dependent to the number of adsorption active sites of the adsorbents” [71, 72]. Linear fitting of experimental data by PFO kinetic model is represented in Fig. 4. Plots in Fig. 4 show straight lines that are not perfect with a coefficient regression equal to 0.42, 0.589, 0.91720, 0.65492, and 0.71797 for walnut shell, coconut shell, peanut shell, and almond shell, respectively. PFO parameters obtained from fitting experimental data are represented in Table 3. From this table, results show a very low R^2 values. In addition, adsorption capacity values determined from curve fitting are far from experimental ones, showing a 43% deviation. This signifies that the adsorption of Cu^{2+} on the four adsorbents does not follow the PFO kinetic model.

Figure 5 shows the application of the PSO kinetic model to the results obtained for the adsorption of Cu^{2+} . It can be observed that all fitting lines match almost perfectly experimental data. Parameters from the PSO kinetic model along with the regression coefficients for the four adsorbents are listed in Table 4. From results in Table 4, it appears that R^2 values are all close to 1, and significantly higher than those of the PFO model. In addition, the fitted adsorption capacity values at equilibrium (Q_e) are 69.73, 33.15, 72.35, and 37.95 mg/g for walnut shell, almond shell, coconut shell, peanut shell, respectively, which are close to experimental

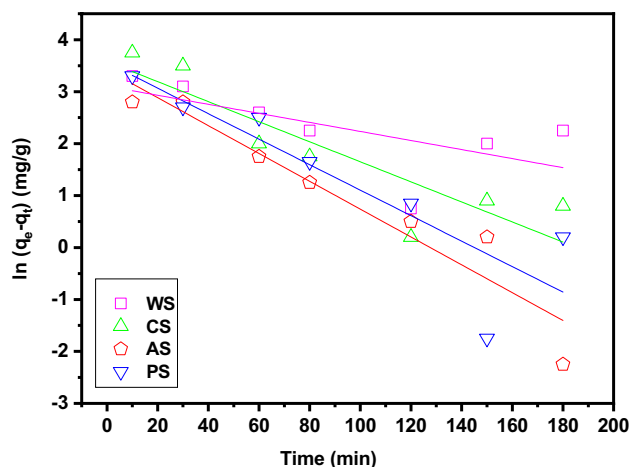


Fig. 4 Pseudo-first order model relating to adsorption kinetics of Cu^{2+} on adsorbents

Table 3 First-order kinetic model parameters for the copper ions adsorption onto investigated samples

Adsorbents	Walnut shell	Almond shell	Coconut shell	Peanut shell
R^2	0.42589	0.91272	0.65492	0.71797
K_1 (min^{-1})	0.00935	0.02761	0.02351	0.02573
Q_m (mg g^{-1})	65.10	24.20	57.39	26.14
$Q_{m,exp}$ (mg g^{-1})	21.23	38.05	32.45	43.10
Relative gap (%)	67.38	57.23	43.45	64.88

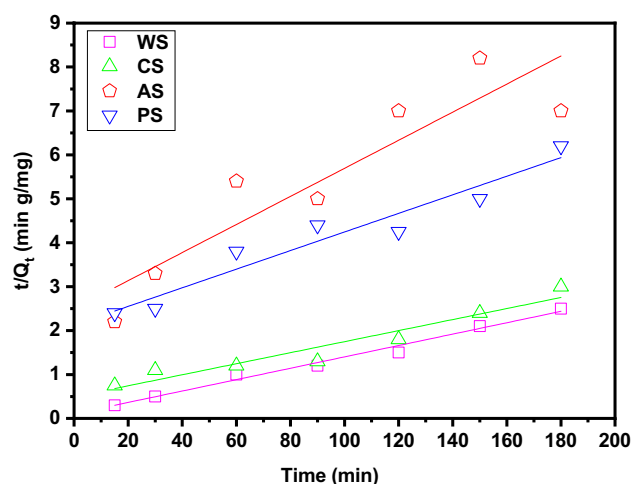


Fig. 5 Pseudo-second order model relating to adsorption kinetics of Cu^{2+} on adsorbents

values. These findings lead to the conclusion that the adsorption process follows the PSO model rather than PFO. It has been found that PSO kinetic model describes well the adsorption process of Cr(VI) on activated carbon prepared from almond shell [73], the adsorption of antibiotic amoxicillin on almond shell ashes [74], the adsorption of Pb(II) on almond shell activated carbon [75], and acid Blue 129 adsorption on almond shell [76], which all support the present results.

3.2.3 Adsorption isotherm

The adsorption isotherm study is an essential approach to describe how the adsorbed molecules distribute at the adsorbent interfaces [77, 78]. Herein, adsorption isotherm studies are conducted by varying adsorbate's concentration from 2×10^{-4} to 4×10^{-3} mol/L with 4×10^{-3} mol/L of Cu^{2+} in 20 mL of solution at pH = 5.5, 25 °C temperature, and equilibrium time of 120 min. The modeling of the adsorption isotherm of Cu^{2+} is then investigated using Langmuir and Freundlich models. The graphical representation of fitting experimental data to Langmuir adsorption isotherm model is shown in Fig. 6. The theoretical curves of Langmuir follow experimental data for the four adsorbents. Therefore, it can be concluded that the adsorption of Cu^{2+} is carried out

Table 4 Second-order kinetic model parameters for the copper ions adsorption onto investigated samples

Adsorbents	Walnut shell	Almond shell	Coconut shell	Peanut shell
R^2	0.98930	0.96739	0.95589	0.94185
K_1 (min ⁻¹)	0.00286	0.00048	0.00042	0.00036
Q_m (mg g ⁻¹)	65.10	24.20	57.39	26.14
$Q_{m,exp}$ (mg g ⁻¹)	69.73	33.15	72.35	37.95
Relative gap (%)	7.11	36.98	26.06	45.17

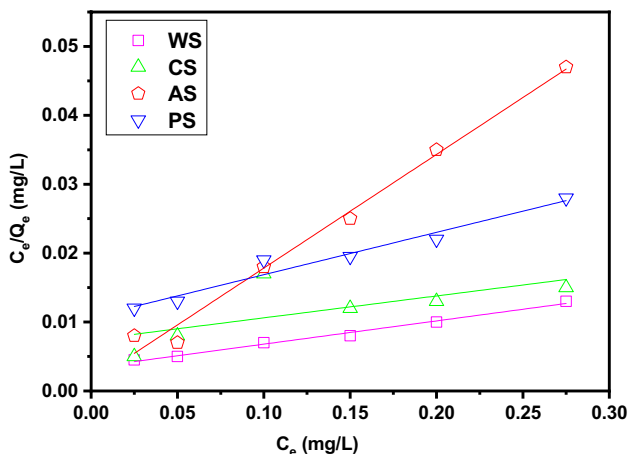


Fig. 6 Langmuir model for adsorption isotherms of Cu²⁺ on adsorbents

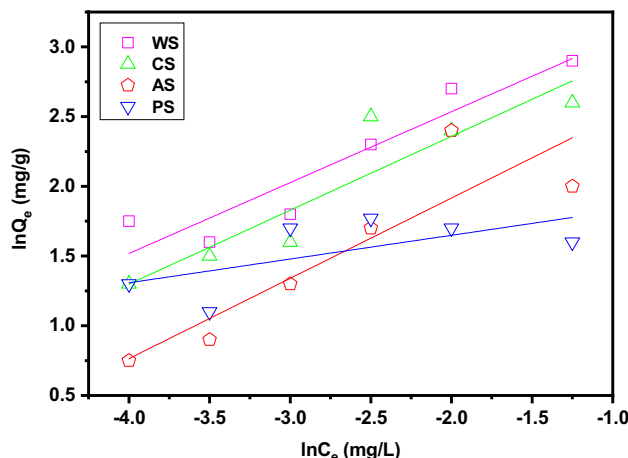


Fig. 7 Freundlich model for adsorption isotherms of Cu²⁺ on adsorbents

Table 5 Langmuir adsorption isotherm parameters for copper adsorption onto investigated samples

Adsorbents	Langmuir model		
	Q_m (mg g ⁻¹)	K_L (L mg ⁻¹)	R^2
Walnut shell	25.6607647	10.8551532	0.9129
Almond shell	5.6980057	115.4605263	0.9707
Coconut shell	18.8040617	10.83095722	0.7689
Peanut shell	10.6394297	13.50431038	0.9462

Table 6 Freundlich adsorption isotherm parameters for copper adsorption onto investigated samples

Adsorbents	Freundlich model		
	K_F (mg g ⁻¹)	$1/n$	R^2
Walnut shell	38.4139241	0.4879	0.8912
Almond shell	20.9458388	0.54762	0.8107
Coconut shell	45.094938	0.6683	0.6710
Peanut shell	9.27006137	0.2597	0.3513

on sites energetically homogeneous by probably forming a monolayer. Table 5 lists adsorption parameters derived from fitting experimental data. It shows that Cu²⁺ ion adsorption on WS is more significant than others, representing an adsorption capacity of 25.6 mg/g. The graphical representation of the adsorption isotherms of the Freundlich model is shown in Fig. 7, while Freundlich-derived parameters are listed in Table 6. By inspecting Fig. 7 and Table 6, it can be observed that the theoretical straight lines have a large deviation from experimental values, with regression coefficient values (R^2) very low than 1. Based on these remarks, it can be concluded that the Freundlich adsorption isotherm model does not describe the adsorption of Cu²⁺ on four adsorbents. Comparing with Langmuir adsorption isotherm’s results, it can be confirmed that Cu²⁺ adsorption

may be well described by the Langmuir model. In this case, the adsorption process occurs mainly at homogeneous sites at adsorbent surface and forms a monolayer.

3.3 Comparison with other adsorbents

The application of agro-waste materials in wastewater treatment is gaining significant scientific interest. These materials, which are usually discharged into the environment without treatment, have been proven as excellent adsorbents for heavy metals and organic pollutants. A large body of literature can be found on agricultural wastes for heavy metals removal. Table 7 lists some studies using agro-wastes and other adsorbents for Cu²⁺ removal along with some

Table 7 Copper sorption capacities of some adsorbents reported in the literature

Adsorbent	Sorption capacity	pH	Equilibrium time (min)	Reference
	(mg/g) of Cu ²⁺			
Soybean hulls	38.70	5	120	[79]
Carrot residue	32.74	4.5	70	[40]
Sugar beet pulp	30.90	4	180	[80]
Apple wastes	10.80	5.9	1440	[42]
Banana peel	4.75	4.5	45	[43]
Walnut shell	6.74	6	120	[81]
Hazelnut shell	6.65	6	120	[81]
Almond shell	3.62	6	120	[81]
Sulfonated multi-walled carbon nanotubes (s-MWCNTs)	59.6	5	360	[82]
purified multi-walled carbon nanotubes (p-MWCNTs)	37.5	5	360	[82]
Hydrogen-bonded metal–organic framework (MOF)	379.13	6	120	[83]
GN/c-MWCNT	38.8	5	60	[84]
Chitosan-GO composite	70	5.1	600	[85]
Walnut shell	25.66	5.5	120	This study
Almond shell	5.69	5.5	120	This study
Peanut shell	10.63	5.5	120	This study
Coconut shell	18.80	5.5	120	This study

experimental conditions. From data reported in Table 7, it can be noticed that hard shells have lower Cu²⁺ adsorption ability compared to soft waste such as apple carrot. The difference is mainly attributed to the adsorbent's surface area and functional groups. The chemical composition of an adsorbent is a key factor in its adsorption performance. On the other hand, some other adsorbents such as carbon nanotubes, MOFs, and composite materials showed very higher adsorption capacities than agro-wastes. This is mainly due to the well-designed structures of synthesized adsorbents, which are intended for a specific purpose. However, given the synthesis cost, the application of agro-wastes seems more beneficial than materials that require high resources. Overall, WS, PS, and CS show an interesting sorption capacity under present conditions compared to previously published works, while AS represents a lower sorption capacity.

3.4 Copper adsorption mechanism on tested materials

The tested materials consist of three components: cellulose, hemicellulose, and lignin. Cellulose has a linear polymeric structure composed of glucose molecules (35 to 50% of the terrestrial plant biomass). Hemicellulose is a branched heterogeneous polymer consisting of chains from several sugars (30 to 45%). Lignin is a group of chemical compounds belonging to phenolic compounds (15–25%). Therefore, the agricultural waste materials contain a complex mixture containing lignin and cellulose as the main constituents.

Chemical adsorption of pollutants can occur through the polar functional groups of lignin and cellulose, including alcohols, acids, phenolic hydroxides, and ethers that act as chemical binding agents [32]. To get more insights on the adsorption mechanism of Cu²⁺, FT-IR structural characterization of adsorbents before and after adsorption was carried out; the results are shown in Fig. 8.

The FTIR spectra recorded in the spectral domain 400–4000 cm⁻¹ for the four adsorbents show the presence of several bands at 3420, 2920, 1730, 1630, 1250, 1046, and 600 cm⁻¹. FTIR spectra recorded in the 4000–2000 cm⁻¹ region show a wide band around 3420 cm⁻¹, which is associated to the vibration of -OH. Bands between 4000 and 3200 cm⁻¹ are assigned to the symmetrical elongation of water, which is formed by the interaction between hydroxyl groups (-OH) and water molecules physisorbed on the metal cation.

It also refers to the N–H vibration of amines, which occurs between 3500 and 3000 cm⁻¹. The valence vibrations in C–H of alcohols observed around 2920 cm⁻¹ are sensitive to the electronic state of the oxygen atom and are therefore disturbed by its interactions with other atoms.

Bands located between 1700 and 1725 cm⁻¹ are attributed to the C=O carbonyl group of acids. The bands located between 1600 and 1670 cm⁻¹ are characteristic of the amine and acetamide groups, respectively. In the 1300–400 cm⁻¹ region, there is a band around 1250 cm⁻¹ attributed to the C–O valence vibration of alcohol. The bands between 1150 and 1000 cm⁻¹ are assigned to the CO vibration of alcohol

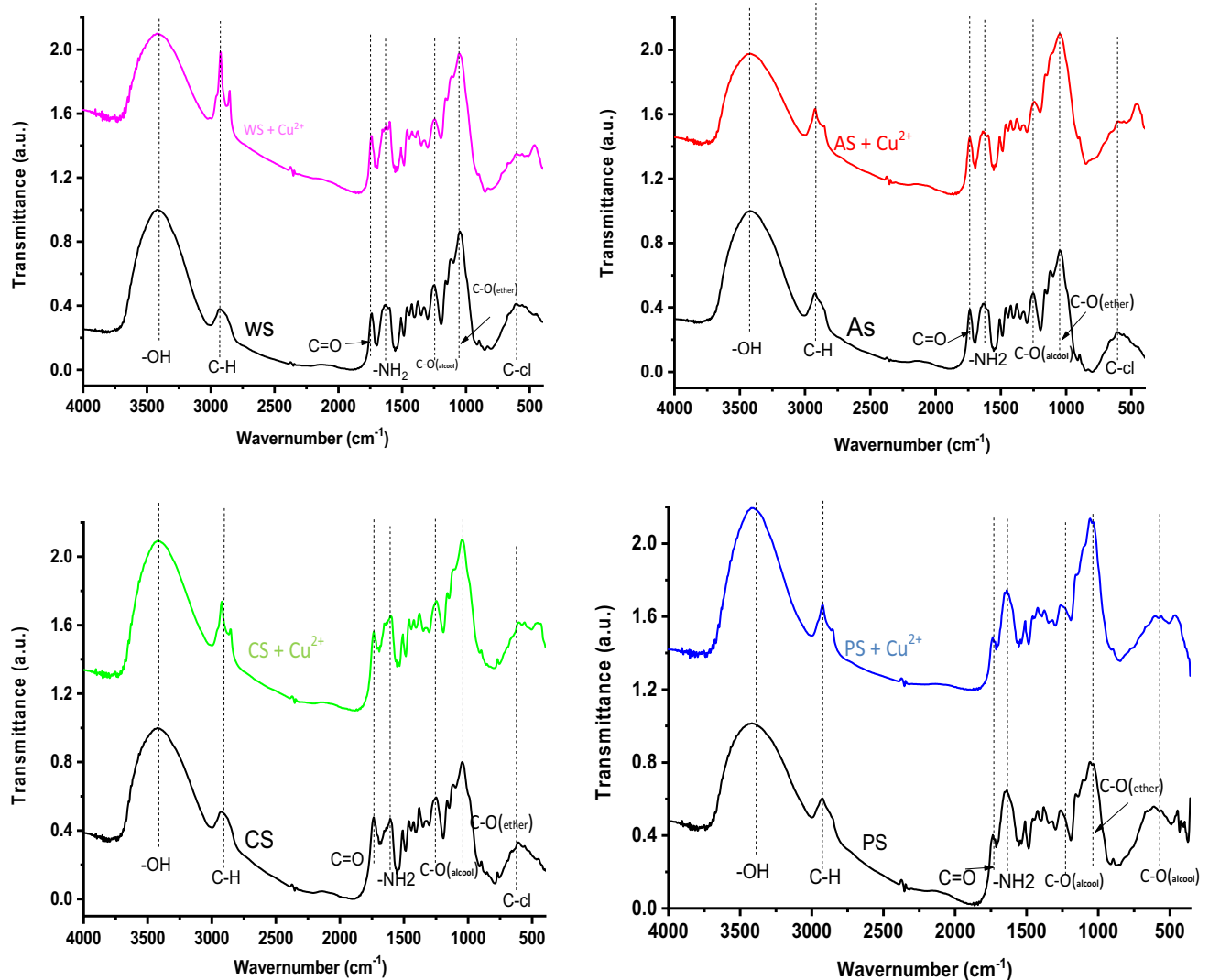


Fig. 8 FTIR spectrum of adsorbents before and after Cu^{2+} adsorption

and cyclic ethers. The 1000–400 cm^{-1} region of the FTIR spectra is characteristic of polymer chains' valence and deformation vibrations. The position of different bands remains unchanged under the experimental conditions.

According to SEM analysis, adsorbents' surface has a rigorous morphology that contains ramifications and cavities, which can be potential sites for Cu^{2+} adsorption. On the other hand, the chemical composition analysis of tested adsorbents reveals a dominant presence of alcohol function. As these chemical functional groups contain a free electron pair on oxygen, it can act as an electronegative adsorption site, thus attracting more Cu^{2+} . Furthermore, cellulose and hemicellulose include ether functions. Lignin has very electron-rich centers with nucleophilic characters represented by aromatic nuclei and carbonyl $\text{C}=\text{O}$ acid function. Therefore, given the electropositive nature of Cu^{2+} , strong physical interactions can be expected between those functional

groups of adsorbents and Cu^{2+} . The mechanism of Cu^{2+} adsorption by these surfaces can be explained by a cooperative fixation of Cu^{2+} by the nucleophilic sites of the three constituents, i.e., cellulose, hemicellulose, and lignin. A previous work investigating the Cu^{2+} adsorption on seaweed-derived biochar has also concluded that the Cu^{2+} adsorption mechanism is due to electrostatic (cationic and anionic) attractions, surface precipitation, and pore depositions [86].

The Cu^{2+} mainly adsorbs on the waste materials' surface by physical interactions without any effect on the bonds as shown by the IR spectra of the surfaces before and after adsorption (Fig. 9). The difference in the adsorption capacity can be explained on the one hand by the specific surface area of each waste which is linked to the particle size and texture of the surface and on the other hand by the number of oxygen atoms carrying the active lone electron pair. Thus, the high retention of the pollutant can be attributed to the

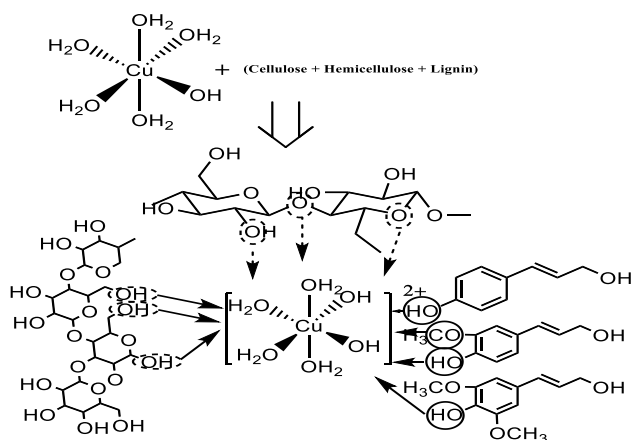


Fig. 9 Representation of all reactive sites from oxygen functions and a proposed adsorption mechanism

high content of cellulose-rich in lone electron pair and the low content of lignin, which is known by its rigidity, impermeability to water, and high resistance to decomposition.

4 Conclusion

Agro-wastes from coconut, almond, walnut, and peanut shells were investigated for adsorption removal of Cu^{2+} from aqueous solutions. Batch adsorption tests were carried out at optimized experimental conditions; pH = 5.5, equilibrium time of 120 min, 50 mg of adsorbent, and 4×10^{-3} mol/L of Cu^{2+} in 20 mL of solution at 25 °C temperature. From kinetic study, the PSO was found the most suitable for describing the kinetics of adsorption of Cu^{2+} on the four adsorbents. On the other hand, Langmuir and Freundlich isotherm models were analyzed, and Langmuir's linear model was found suitable for describing Cu^{2+} adsorption process on the four adsorbents. The FTIR study has shown that the adsorbents' chemical composition is dominant by C=O, C–O–C, and O–H functional groups. The adsorption of Cu^{2+} occurred through interactions between lone electron pair of functional groups of adsorbents and Cu^{2+} , without occurrence of any chemical interactions. Results from the present work highlight the urgent need for the valorization of agro-wastes as a source of adsorbents. In the next works, further efforts will be devoted to valorizing these agro-wastes and their various uses in value-added applications such as energy and biofuels.

Supplementary Information The online version contains supplementary material available at <https://doi.org/10.1007/s13399-022-02564-4>.

Funding The authors would like to thank the Deanship of Scientific Research at Umm Al-Qura University for supporting this work by Grant Code: 20- SCI-1-01-0006.

Declarations

Conflict of interest The authors declare no competing interests.

References

- Wang F, Pan Y, Cai P et al (2017) Single and binary adsorption of heavy metal ions from aqueous solutions using sugarcane cellulose-based adsorbent. *Biores Technol* 241:482–490
- Periyasamy S, Kumar IA, Viswanathan N (2020) Activated carbon from different waste materials for the removal of toxic metals. In: *Green materials for wastewater treatment*. Springer, pp 47–68
- Ihsanullah AA, Al-Amer AM et al (2016) Heavy metal removal from aqueous solution by advanced carbon nanotubes: critical review of adsorption applications. *Sep Purif Technol* 157:141–161. <https://doi.org/10.1016/j.seppur.2015.11.039>
- Varsha M, Senthil Kumar P, SenthilRathi B (2022) A review on recent trends in the removal of emerging contaminants from aquatic environment using low-cost adsorbents. *Chemosphere* 287:132270. <https://doi.org/10.1016/j.chemosphere.2021.132270>
- Xu L, Suo H, Liu R (2021) Preparation and characterization of magnetic bioadsorbent for adsorption of Cd (II) ions. *J Indian Chem Soc* 98:100111
- Salih SS, Ghosh TK (2017) Preparation and characterization of bioadsorbent beads for chromium and zinc ions adsorption. *Cogent Environ Sci* 3:1401577
- Raut PN, Gotmare SR (2019) adsorption of Cu ions from wastewater by natural medicinal Bioadsorbent. *Inter J Res App Sci & Eng Tech* 7:876
- He L, Yang C, Ding J et al (2022) Fe, N-doped carbonaceous catalyst activating periodate for micropollutant removal: significant role of electron transfer. *Appl Catal B* 303:120880. <https://doi.org/10.1016/j.apcatb.2021.120880>
- Zhang L, Wang L, Zhang Y et al (2022) The performance of electrode ultrafiltration membrane bioreactor in treating cosmetics wastewater and its anti-fouling properties. *Environ Res* 206:112629. <https://doi.org/10.1016/j.envres.2021.112629>
- Chakraborty R, Asthana A, Singh AK et al (2022) Adsorption of heavy metal ions by various low-cost adsorbents: a review. *Int J Environ Anal Chem* 102:342–379. <https://doi.org/10.1080/03067319.2020.1722811>
- Bilal M, Ihsanullah I, Younas M, Ul Hassan Shah M (2021) Recent advances in applications of low-cost adsorbents for the removal of heavy metals from water: a critical review. *Sep Purif Technol* 278:119510. <https://doi.org/10.1016/j.seppur.2021.119510>
- Shi C, Wu Z, Yang F, Tang Y (2021) Janus particles with pH switchable properties for high-efficiency adsorption of PPCPs in water. *Solid State Sci* 119:106702. <https://doi.org/10.1016/j.solidstatesciences.2021.106702>
- Liu W, Li J, Zheng J et al (2020) Different Pathways for Cr(III) Oxidation: implications for Cr(VI) Reoccurrence in Reduced Chromite Ore Processing Residue. *Environ Sci Technol* 54:11971–11979. <https://doi.org/10.1021/acs.est.0c01855>
- Sud D, Mahajan G, Kaur MP (2008) Agricultural waste material as potential adsorbent for sequestering heavy metal ions from aqueous solutions — a review. *Biores Technol* 99:6017–6027. <https://doi.org/10.1016/j.biortech.2007.11.064>
- Saheed IO, Oh WD, Suah FBM (2021) Chitosan modifications for adsorption of pollutants — a review. *J Hazard Mater* 408:124889. <https://doi.org/10.1016/j.jhazmat.2020.124889>

16. Awad AM, Shaikh SMR, Jalab R et al (2019) Adsorption of organic pollutants by natural and modified clays: a comprehensive review. *Sep Purif Technol* 228:115719. <https://doi.org/10.1016/j.seppur.2019.115719>
17. Dai Y, Zhang N, Xing C et al (2019) The adsorption, regeneration and engineering applications of biochar for removal organic pollutants: a review. *Chemosphere* 223:12–27. <https://doi.org/10.1016/j.chemosphere.2019.01.161>
18. Ihsanullah I, Jamal A, Ilyas M et al (2020) Bioremediation of dyes: current status and prospects. *J Water Process Eng* 38:101680. <https://doi.org/10.1016/j.jwpe.2020.101680>
19. Omer AM, Dey R, Eltaweil AS et al (2022) Insights into recent advances of chitosan-based adsorbents for sustainable removal of heavy metals and anions. *Arab J Chem* 15:103543. <https://doi.org/10.1016/j.arabjc.2021.103543>
20. Gupta G, Khan J, Singh NK (2021) Application and efficacy of low-cost adsorbents for metal removal from contaminated water: a review. *Mater Today Proc* 43:2958–2964. <https://doi.org/10.1016/j.matpr.2021.01.316>
21. Bilal M, Ihsanullah I, Ul Hassan Shah M, Younas M (2021) Enhanced removal of cadmium from water using bio-sorbents synthesized from branches and leaves of *Capparis decidua* and *Ziziphus mauritiana*. *Environ Technol Innov* 24:101922. <https://doi.org/10.1016/j.eti.2021.101922>
22. Olabanji IO, Oluoyemi EA (2021) Investigating the effectiveness of raw okra (*Abelmoschus esculentus* L) and raw sugarcane (*Saccharum officinarum*) wastes as bioadsorbent of heavy metal in aqueous systems. *Modern Adv Geogr Environ Earth Sci* 6:50–58
23. Liu Y, Li X, Zhou J, He W (2019) Preparation and characterization of *Camellia oleifera* nut shell-based bioadsorbent and its application for heavy metals removal. *BioResources* 14:234–250
24. Hernández-Cocolezzi H, Salinas RA, Águila-Almanza E et al (2020) Natural hydroxyapatite from fishbone waste for the rapid adsorption of heavy metals of aqueous effluent. *Environ Technol Innov* 20:101109
25. Guo S, Jiao P, Dan Z et al (2017) Synthesis of magnetic bioadsorbent for adsorption of Zn (II), Cd (II) and Pb (II) ions from aqueous solution. *Chem Eng Res Des* 126:217–231
26. de Andrade Neto JC, Pereira GJ, Morandim-Giannetti AdeA (2020) Chitosan and corn stover derivative bioadsorbent: characterization and application in hexavalent chromium adsorption processes. *Cellulose* 27:6317–6331
27. Janyasuthiwong S, Phiri SM, Kijjanapanich P et al (2015) Copper, lead and zinc removal from metal-contaminated wastewater by adsorption onto agricultural wastes. *Environ Technol* 36:3071–3083. <https://doi.org/10.1080/09593330.2015.1053537>
28. Alalwan HA, Kadhom MA, Alminshid AH (2020) Removal of heavy metals from wastewater using agricultural byproducts. *J Water Supply Res Technol AQUA* 69:99–112. <https://doi.org/10.2166/aqua.2020.133>
29. Tsade H, Murthy HA, Muniswamy D (2020) Bio-sorbents from agricultural wastes for eradication of heavy metals: a review. *J Mater Environ Sci* 11:1719–1735
30. Nieva AD, Camus REE, Halabasco ER, Doma BT (2020) Prediction of adsorptive capacity of various agricultural wastes in the removal of heavy metals dyes and antibiotic in wastewater using ANN. *Int J Environ Sci Dev* 11
31. Ibrahim BM (2021) Heavy metal ions removal from wastewater using various low-cost agricultural wastes as adsorbents: a survey. *Zanco J Pure Appl Sci* 33:76–91
32. Minkova V, Razvigorova M, Bjornbom E et al (2001) Effect of water vapour and biomass nature on the yield and quality of the pyrolysis products from biomass. *Fuel Process Technol* 70:53–61. [https://doi.org/10.1016/S0378-3820\(00\)00153-3](https://doi.org/10.1016/S0378-3820(00)00153-3)
33. Šćiban M, Klačnja M, Škrbić B (2008) Adsorption of copper ions from water by modified agricultural by-products. *Desalination* 229:170–180
34. Kahraman S, Dogan N, Erdemoglu S (2008) Use of various agricultural wastes for the removal of heavy metal ions. *Int J Environ Pollut* 34:275–284
35. Bandela NN, Babrekar M, Jogdand O, Kaushik G (2016) Removal of copper from aqueous solution using local agricultural wastes as low cost adsorbent. *J Mater Environ Sci* 7:1972–1978
36. Al Bsoul A, Zeatoun L, Abdelhay A, Chiha M (2014) Adsorption of copper ions from water by different types of natural seed materials. *Desalin Water Treat* 52:5876–5882
37. Guibal E (2004) Interactions of metal ions with chitosan-based sorbents: a review. *Sep Purif Technol* 38:43–74. <https://doi.org/10.1016/j.seppur.2003.10.004>
38. Boukhelif F, Bencheikh A, Ahlafi H (2011) Characterisation and adsorption propriety of chitin treated at high temperature Carac-terisation et proprietes d'adsorption de la chitine traitee a haute temperature. *Phys Chem News* 58:67–72
39. Fatima B (2020) Quantitative Analysis by IR: Determination of Chitin/Chitosan DD. *Mod Spectrosc Techn Appl*. <https://doi.org/10.5772/intechopen.89708>
40. Nasernejad B, Zadeh TE, Pour BB et al (2005) Comparison for biosorption modeling of heavy metals (Cr (III), Cu (II), Zn (II)) adsorption from wastewater by carrot residues. *Process Biochem* 40:1319–1322. <https://doi.org/10.1016/j.procbio.2004.06.010>
41. Marshall WE, Champagne ET (1995) Agricultural byproducts as adsorbents for metal ions in laboratory prepared solutions and in manufacturing wastewater. *J Environ Sci Health A Environ Sci Eng Toxicol* 30:241–261. <https://doi.org/10.1080/10934529509376198>
42. Lee SH, Jung CH, Chung H et al (1998) Removal of heavy metals from aqueous solution by apple residues. *Process Biochem* 33:205–211. [https://doi.org/10.1016/S0032-9592\(97\)00055-1](https://doi.org/10.1016/S0032-9592(97)00055-1)
43. Low KS, Lee CK, Leo AC (1995) Removal of metals from electroplating wastes using banana pith. *Biores Technol* 51:227–231. [https://doi.org/10.1016/0960-8524\(94\)00123-1](https://doi.org/10.1016/0960-8524(94)00123-1)
44. Shukla SR, Pai RS (2005) Adsorption of Cu(II), Ni(II) and Zn(II) on dye loaded groundnut shells and sawdust. *Sep Purif Technol* 43:1–8. <https://doi.org/10.1016/j.seppur.2004.09.003>
45. Villaescusa I, Fiol N, Martínez M et al (2004) Removal of copper and nickel ions from aqueous solutions by grape stalks wastes. *Water Res* 38:992–1002. <https://doi.org/10.1016/j.watres.2003.10.040>
46. Basci N, Kocadagistan E, Kocadagistan B (2004) Biosorption of copper (II) from aqueous solutions by wheat shell. *Desalination* 164:135–140. [https://doi.org/10.1016/S0011-9164\(04\)00172-9](https://doi.org/10.1016/S0011-9164(04)00172-9)
47. Çay S, Uyanik A, Özaşık A (2004) Single and binary component adsorption of copper(II) and cadmium(II) from aqueous solutions using tea-industry waste. *Sep Purif Technol* 38:273–280. <https://doi.org/10.1016/j.seppur.2003.12.003>
48. Sun G, Shi W (1998) Sunflower stalks as adsorbents for the removal of metal ions from wastewater. *Ind Eng Chem Res* 37:1324–1328. <https://doi.org/10.1021/ie970468j>
49. Ho YS (2003) Removal of copper ions from aqueous solution by tree fern. *Water Res* 37:2323–2330. [https://doi.org/10.1016/S0043-1354\(03\)00002-2](https://doi.org/10.1016/S0043-1354(03)00002-2)
50. Özcan A, Özcan AS, Tunali S et al (2005) Determination of the equilibrium, kinetic and thermodynamic parameters of adsorption of copper(II) ions onto seeds of *Capsicum annum*. *J Hazard Mater* 124:200–208. <https://doi.org/10.1016/j.jhazmat.2005.05.007>
51. Ho YS, Ofomaja AE (2006) Kinetic studies of copper ion adsorption on palm kernel fibre. *J Hazard Mater* 137:1796–1802. <https://doi.org/10.1016/j.jhazmat.2006.05.023>

52. Altun T, Pehlivan E (2007) Removal of copper (II) ions from aqueous solutions by walnut, hazelnut and almond shells. *Clean Soil Air Water* 35:601–606
53. Liu H, Wang Y, Li Q et al (2022) Research on the evolution characteristics of oxygen-containing functional groups during the combustion process of the torrefied corn stalk. *Biomass Bioenergy* 158:106343. <https://doi.org/10.1016/j.biombioe.2022.106343>
54. Yang H, Yan R, Chen H et al (2007) Characteristics of hemicellulose, cellulose and lignin pyrolysis. *Fuel* 86:1781–1788
55. Chen B, Zhou D, Zhu L (2008) Transitional adsorption and partition of nonpolar and polar aromatic contaminants by biochars of pine needles with different pyrolytic temperatures. *Environ Sci Technol* 42:5137–5143
56. Li G, Huang S, Zhu N et al (2021) Defect-rich heterojunction photocatalyst originated from the removal of chloride ions and its degradation mechanism of norfloxacin. *Chem Eng J* 421:127852. <https://doi.org/10.1016/j.cej.2020.127852>
57. Urruzola I, Robles E, Serrano L, Labidi J (2014) Nanopaper from almond (*Prunus dulcis*) shell. *Cellulose* 21:1619–1629. <https://doi.org/10.1007/s10570-014-0238-y>
58. Ertaş M, Alma MH (2010) Pyrolysis of laurel (*Laurus nobilis* L.) extraction residues in a fixed-bed reactor: Characterization of bio-oil and bio-char. *J Anal Appl Pyrol* 88:22–29
59. Kurosaki F, Koyanaka H, Hata T, Imamura Y (2007) Macroporous carbon prepared by flash heating of sawdust. *Carbon (New York, NY)* 45:671–673
60. Malika A, Jacques N, Jaafar EF et al (2016) Pyrolysis investigation of food wastes by TG-MS-DSC technique. *Biomass Conversion Biorefinery* 6:161–172
61. Cruz G, Rodrigues AdALP, da Silva DF, Gomes WC (2021) Physical–chemical characterization and thermal behavior of cassava harvest waste for application in thermochemical processes. *J Therm Anal Calorim* 143:3611–3622. <https://doi.org/10.1007/s10973-020-09330-6>
62. Ahmadou A, Napoli A, Durand N, Montet D (2019) High physical properties of cashew nut shell biochars in the adsorption of mycotoxins. *Inter J Food Res* 6:18
63. Ahmadou A, Brun N, Napoli A et al (2019) Effect of pyrolysis temperature on ochratoxin A adsorption mechanisms and kinetics by cashew nut shell biochars. *SRDP J Food Sci Tech* 4:877
64. Annab H, Fiol N, Villaescusa I, Essamri A (2019) A proposal for the sustainable treatment and valorisation of olive mill wastes. *J Environ Chem Eng* 7:102803. <https://doi.org/10.1016/j.jece.2018.11.047>
65. Bautista-Toledo I, Ferro-García MA, Rivera-Utrilla J et al (2005) Bisphenol A removal from water by activated carbon. Effects of carbon characteristics and solution chemistry. *Environ Sci Technol* 39:6246–6250. <https://doi.org/10.1021/es0481169>
66. Yu B, Zhang Y, Shukla A et al (2000) The removal of heavy metal from aqueous solutions by sawdust adsorption — removal of copper. *J Hazard Mater* 80:33–42. [https://doi.org/10.1016/S0304-3894\(00\)00278-8](https://doi.org/10.1016/S0304-3894(00)00278-8)
67. Vishnu D, Dhandapani B, Ramakrishnan SR et al (2021) Fabrication of surface-engineered superparamagnetic nanocomposites (Co/Fe/Mn) with biochar from groundnut waste residues for the elimination of copper and lead metal ions. *J Nanostruct Chem* 11:215–228. <https://doi.org/10.1007/s40097-020-00360-y>
68. Vishnu D, Dhandapani B (2021) Synthesis of novel adsorbent by incorporation of plant extracts in amino-functionalized silica-coated magnetic nanomaterial for the removal of Zn²⁺ and Cu²⁺ from aqueous solution. *J Environ Health Sci Eng* 19:1413–1424. <https://doi.org/10.1007/s40201-021-00696-9>
69. Lagergren S (1898) Zur theorie der sogenannten adsorption gelöster stoffe. *Handlingar* 24:1
70. Ho YS, McKay G (1999) Pseudo-second order model for sorption processes. *Process Biochem* 34:451–465. [https://doi.org/10.1016/S0032-9592\(98\)00112-5](https://doi.org/10.1016/S0032-9592(98)00112-5)
71. Ganesan P, Lakshmi J, Sozhan G, Vasudevan S (2013) Removal of manganese from water by electrocoagulation: adsorption, kinetics and thermodynamic studies. *Can J Chem Eng* 91:448–458. <https://doi.org/10.1002/cjce.21709>
72. Badawi MA, Negm NA, Abou Kana MTH et al (2017) Adsorption of aluminum and lead from wastewater by chitosan-tannic acid modified biopolymers: isotherms, kinetics, thermodynamics and process mechanism. *Int J Biol Macromol* 99:465–476. <https://doi.org/10.1016/j.ijbiomac.2017.03.003>
73. Rai MK, Giri BS, Nath Y et al (2018) Adsorption of hexavalent chromium from aqueous solution by activated carbon prepared from almond shell: kinetics, equilibrium and thermodynamics study. *J Water Supply Res Technol AQUA* 67:724–737. <https://doi.org/10.2166/aqua.2018.047>
74. Homem V, Alves A, Santos L (2010) Amoxicillin removal from aqueous matrices by sorption with almond shell ashes. *Int J Environ Anal Chem* 90:1063–1084. <https://doi.org/10.1080/03067310903410964>
75. Thitame PV, Shukla SR (2017) Removal of lead (II) from synthetic solution and industry wastewater using almond shell activated carbon. *Environ Prog Sustainable Energy* 36:1628–1633. <https://doi.org/10.1002/ep.12616>
76. Fat'hi MR, Asfaram A, Hadipour A, Roosta M (2014) Kinetics and thermodynamic studies for removal of acid blue 129 from aqueous solution by almond shell. *J Environ Health Sci Eng* 12:62. <https://doi.org/10.1186/2052-336X-12-62>
77. Vishnu D, Dhandapani B, Vaishnavi G, Preethi V (2022) Synthesis of tri-metallic surface engineered nanobiochar from cynodon dactylon residues in a single step — batch and column studies for the removal of copper and lead ions. *Chemosphere* 286:131572. <https://doi.org/10.1016/j.chemosphere.2021.131572>
78. Vishnu D, Dhandapani B, Santhiya K (2021) The symbiotic effect of integrated *Muraya koenigii* extract and surface-modified magnetic microspheres — a green biosorbent for the removal of Cu(II) and Cr(VI) ions from aqueous solutions. *Chem Eng Commun* 208:851–862. <https://doi.org/10.1080/00986445.2019.1691538>
79. Marshall WE, Champagne ET (1995) Agricultural byproducts as adsorbents for metal ions in laboratory prepared solutions and in manufacturing wastewater. *J Environ Sci Health A* 30:241–261
80. Aksu Z, İsoğlu İA (2005) Removal of copper (II) ions from aqueous solution by biosorption onto agricultural waste sugar beet pulp. *Process Biochem* 40:3031–3044
81. Altun T, Pehlivan E (2007) Removal of copper (II) ions from aqueous solutions by walnut-, hazelnut- and almond-shells. *Clean Soil Air Water* 35:601–606
82. Ge Y, Li Z, Xiao D et al (2014) Sulfonated multi-walled carbon nanotubes for the removal of copper (II) from aqueous solutions. *J Ind Eng Chem* 20:1765–1771. <https://doi.org/10.1016/j.jiec.2013.08.030>
83. Yu C, Shao Z, Liu L, Hou H (2018) Efficient and selective removal of copper(II) from aqueous solution by a highly stable hydrogen-bonded metal–organic framework. *Cryst Growth Des* 18:3082–3088. <https://doi.org/10.1021/acs.cgd.8b00224>
84. Yusuf M, Khan MA, Abdullah EC et al (2016) Dodecyl sulfate chain anchored mesoporous graphene: Synthesis and application to sequester heavy metal ions from aqueous phase. *Chem Eng J* 304:431–439. <https://doi.org/10.1016/j.cej.2016.06.109>
85. Chen Y, Chen L, Bai H, Li L (2013) Graphene oxide–chitosan composite hydrogels as broad-spectrum adsorbents for water purification. *J Mater Chem A* 1:1992–2001. <https://doi.org/10.1039/C2TA00406B>
86. Katiyar R, Patel AK, Nguyen T-B et al (2021) Adsorption of copper (II) in aqueous solution using biochars derived from *Ascophyllum nodosum* seaweed. *Biores Technol* 328:124829. <https://doi.org/10.1016/j.biortech.2021.124829>

Publisher's note Springer Nature remains neutral with regard to jurisdictional claims in published maps and institutional affiliations.